miR-140-3p enhances cisplatin sensitivity and attenuates stem cell-like properties through repressing Wnt/β-catenin signaling in lung adenocarcinoma cells

SHUOMING WU[1], HAORAN WANG[2], YINPENG PAN[1], XIANGBAO YANG[1] and DUOGUANG WU[3]

[1]Department of Thoracic Surgery, The First People's Hospital of Lianyungang, Lianyungang, Jiangsu 222000;
[2]Department of Thoracic Surgery, The Affiliated Cancer Hospital of Zhengzhou University, Zhengzhou, Henan 450008;
[3]Department of Thoracic Surgery, Sun Yat-Sen Memorial Hospital, Sun Yat-Sen University, Guangzhou, Guangdong 510120, P.R. China

Received November 4, 2019; Accepted April 9, 2020

DOI: 10.3892/etm.2020.8847

Abstract. Lung adenocarcinoma (LUAD) is the most predominant subtype of non-small cell lung cancer (NSCLC) that is experiencing the fastest growth rate in incidence. Chemoresistance and the presence of cancer stem cells are considered to be the main obstacles preventing the successful treatment of patients with NSCLC, the molecular mechanism of which remains poorly understood. The present study aimed to investigate the effects of microRNA (miR)-140-3p on cisplatin sensitivity and stem cell-like properties of LUAD cells. Analysis of publicly available data demonstrated that miR-140-3p expression was downregulated in LUAD, and positively associated with the overall survival rate of patients. In addition, transfection with the miR-140-3p mimic reduced LUAD cell viability and induced apoptosis following treatment with cisplatin whilst decreasing stem cell-like properties. miR-140-3p overexpression was also found to attenuate cisplatin resistance and reduce stem cell-like properties in LUAD cells by suppressing Wnt/β-catenin signaling, all of which were reversed by the overexpression of β-catenin. Taken together, results of the present study suggest miR-140-3p to be an effective therapeutic strategy for patients with LUAD.

Introduction

Lung cancer remains to be the leading cause of cancer-associated mortality worldwide, where the rate of incidence continues increasing (1). According to the GLOBOCAN reports, the incidence of lung cancer stood at 2.1 million occurred worldwide as of 2018, compared with 1.8 million in 2012 (2,3). Non-small cell lung cancer (NSCLC) is the predominant type of lung cancer, accounting for ~80% of all reported cases (4). Recently, lung adenocarcinoma (LUAD) has been reported to be the most predominant subtype of NSCLC that is experiencing the fastest growth in incidence (5). Cisplatin is used extensively as the front-line treatment option for NSCLC and has been reported to improve the survival outcomes of patients by impairing the structure and function of DNA in cancer cells (6). However, its efficacy is frequently hindered by the development of chemoresistance (7). Tumor cells that are resistant to chemotherapy exhibit characteristics of malignant behavior, including high proliferative capability and potent antiapoptotic ability (8,9). Although studies on cisplatin resistance have been performed previously (10-12), the molecular mechanism underlying tumor drug resistance remains poorly understood.

Over the past number of decades, cancer stem cells (CSCs) have attracted widespread attention due to their capabilities of self-renewal and differentiation during cellular stress or drug resistance (13,14). CSCs have been reported in several types of human cancer, including LUAD (15,16). Cluster of differentiation 133 (CD133) has been previously demonstrated to be a key marker of lung CSCs, which have the ability to grow indefinitely into tumor spheres in serum-free medium supplemented with epidermal growth factor (EGF) and basal fibroblast growth factor (bFGF) (17). Additionally, high expression levels of pluripotency factors, including SRY-Box 2 (SOX2), Octamer-binding transcription factor 4 (OCT4), Kruppel like factor 4 (KLF4), NANOG and ATP binding cassette subfamily G member 2 (ABCG2) are associated with enhanced cancer stem cell-like properties (18,19). Although CSCs represent a small population of total tumor cells, they serve key roles in tumor initiation, progression and resistance to radiotherapy and chemotherapy (20). Previous studies have reported that CSCs are under the regulation of a number of signaling pathways, including Wnt/β-catenin, Notch and Hedgehog signaling pathways (21,22). Therefore, inhibition of CSCs by targeting

Correspondence to: Dr Duoguang Wu, Department of Thoracic Surgery, Sun Yat-Sen Memorial Hospital, Sun Yat-Sen University, 107 Yanjiang West Road, Guangzhou, Guangdong 510120, P.R. China
E-mail: qwec_158@163.com

Key words: lung adenocarcinoma, micRNA-140-3p, cisplatin, cancer stem cell-like properties, Wnt/β-catenin signaling

the aforementioned signaling pathways may increase the efficacy of lung cancer therapy.

microRNAs (miRNAs/miRs) are a family of short RNAs that do not encode proteins. They negatively regulate gene expression by direct binding to the 3'-untranslated region of their mRNA targets and participate in the regulation of several biological processes, including cancer cell proliferation, apoptosis, sensitivity to chemotherapy and CSCs stemness (23,24). Previous studies have demonstrated several types of miRNAs to be either upregulated or downregulated in lung cancer, contributing to chemoresistance and enhancing stem cell-like properties through regulation of CSC-associated signaling pathways. Wang *et al* (25) reported that miR-181b overexpression attenuated chemoresistance by regulating cancer stem cell-like properties and the Notch signaling pathway in NSCLC. In addition, miR-708-5p has been revealed to suppress stem cell-like phenotypes in lung cancer by repressing the Wnt/β-catenin signaling pathway (26). Previous studies have suggested that upregulated miR-140-3p expression was significantly associated with reduced cell proliferation, invasion, migration and sorafenib resistance in a variety of tumors (27-30). It was also reported previously that miR-140-3p expression was downregulated in lung squamous cell carcinoma (LUSC) (31), where it has been demonstrated to function as a tumor suppressor (32). However, the expression profile and physiological function of miR-140-3p in LUAD remain poorly understood.

The present study aimed to investigate the effects of miR-140-3p on cisplatin sensitivity and stem cell-like properties of LUAD cells and determine the associated molecular mechanisms that may provide potential therapeutic strategies for the treatment of LUAD.

Materials and methods

Bioinformatics analysis. The RNA array dataset GSE74190 obtained from the NCBI/GEO database (https://www.ncbi.nlm.nih.gov/gds/) and RNA seq data from The Cancer Genome Atlas (TCGA) database (https://cancergenome.nih.gov/) were used to analyze the expression of miR-140-3p in LUAD tissues and adjacent tissues and over survival rate of patients with LUAD. The median value of miR-140-3p expression from the TCGA dataset was used to determine 'low' and 'high' expression.

Cell culture. The human bronchial epithelial cell line BEAS-2B and lung adenocarcinoma cell lines A549, H1299, H292 and Calu3 were purchased from the American Type Culture Collection. BEAS-2B cells were cultured at 37˚C in 5% CO_2 in Bronchial Epithelial Basal Medium (Lonza Group Ltd.) supplemented with 10% FBS (HyClone; GE Healthcare Life Sciences), whilst the lung adenocarcinoma cell lines were cultured in RPMI-1640 medium supplemented with 10% FBS and 1% penicillin/streptomycin (Gibco; Thermo Fisher Scientific, Inc.) at 37˚C in 5% CO_2.

Cell transfection. A549 and Calu3 cells were cultured in six-well plates ($8x10^5$ cells/well) and transfected with plasmids (pcDNA3.1-ctnnb1 or pcDNA3.1-vector; Shanghai GenePharma Co., Ltd.) or mimics (miR-140-3p mimics, 5'-UACCACAGGGUAGAACCACGG-3' or control mimics, 5'-GCAAGAGACAAGCGCUUAGCC-3'; Shanghai GenePharma Co., Ltd.), using Lipofectamine® 2000 reagent (Invitrogen; Thermo Fisher Scientific, Inc.). Briefly, the plasmids (2 μg) or mimics (50 nM) were added to 200 μl Opti-MEM medium (Gibco; Thermo Fisher Scientific, Inc.) in one vial, whilst 4 μl Lipofectamine® 2000 was diluted in 200 μl Opti-MEM in another vial. Following incubation for 5 min at room temperature, the contents of both vials were combined and incubated for a further 20 min at room temperature before the mixture was added to the cells. The media in each well was then replaced with fresh medium 6 h following incubation with the transfection mixture at 37˚C. The transfected cells were harvested 48 h later for subsequent experimentation.

Reverse transcription-quantitative PCR (RT-qPCR). Total RNA was extracted from the cultured cells using TRIzol® reagent (Invitrogen; Thermo Fisher Scientific, Inc.), according to the manufacturer's protocol. Total RNA was reverse transcribed into cDNA using the Moloney murine leukemia virus RT kit, with the M-MLV buffer, dNTP and random primers (all from Promega Corporation). The temperature protocol for the reverse transcription reaction consisted of cDNA synthesis at 37˚C for 60 min and termination at 80˚C for 2 min. qPCR was subsequently performed using the SYBR Green Realtime PCR Master Mix (Beijing Solarbio Science & Technology Co., Ltd.) in a Bio-Rad CFX96 system (Bio-Rad Laboratories, Inc.), according to the manufacturer's protocols. The primer sequences used for qPCR were designed and synthesized by Guangzhou RiboBio Co., Ltd. (Table I). The following thermocycling conditions were used for the qPCR: Initial denaturation at 95˚C for 2 min, followed by 40 cycles 94˚C for 20 sec and 60˚C for 30 sec, and final extension at 72˚C for 30 sec. Relative mRNA or miRNA expression levels were calculated using the $2^{-\Delta\Delta Cq}$ method (33) and normalized to the internal reference genes GAPDH and U6, respectively. All experiments were performed in triplicate.

Cell viability assay. After transfection for 48 h, cells were seeded into 96-well plates ($4x10^3$ cells/well) and incubated with RPMI-1640 medium supplemented with 10% FBS and 1% penicillin/streptomycin at 37˚C in 5% CO_2 overnight. Freshly prepared cisplatin (Jiangsu Haosen Pharmaceutical Group Co., Ltd.) was added at the indicated concentrations (0, 1, 2, 4, 6 and 8 μg/ml). After treatment for 24 h at 37˚C in 5% CO_2, cells were incubated with 20 μl MTT reagent (Sigma-Aldrich; Merck KGaA) at 37˚C for 4 h. Following MTT incubation, the purple formazan crystals were dissolved using dimethyl sulfoxide (100 μl/well) and cell viability was subsequently analyzed at a wavelength of 590 nm, using a microplate reader (Bio-Rad Laboratories, Inc.) All experiments were performed in triplicate.

Colony formation assay. After transfection for 48 h, cells were seeded into 24-well plates ($1x10^5$ cells/well) and incubated with RPMI-1640 medium at 37˚C in 5% CO_2 overnight. Subsequently, cells were cultured in RPMI-1640 medium supplemented with cisplatin (5 μg/ml) for 24 h at 37˚C in 5% CO_2. Cell colonies were fixed with pre-cooled

Table I. Primer sequences used for reverse transcription-quantitative PCR.

Primer	Forward (5'-3')	Reverse (5'-3')
OCT-4	GAAGGATGTGGTCCGAGTGT	GTGAAGTGAGGGCTCCCATA
SOX-2	ACACCAATCCCATCCACACT	GCAAACTTCCTGCAAAGCTC
KLF-4	ACCCACACAGGTGAGAAACC	ATGTGTAAGGCGAGGTGGTC
NANOG	TTCCTTCCTCCATGGATCTG	ATCTGCTGGAGGCTGAGGTA
ABCG2	GTGGCCTTGGCTTGTATGAT	AACAATTGCTGCTGTGCAAC
GAPDH	AACGGATTTGGTCGTATTG	GGAAGATGGTGATGGGATT
β-catenin	AAAGCGGCTGTTAGTCACTGG	CGAGTCATTGCATACTGTCCAT
c-Myc	GGCTCCTGGCAAAAGGTCA	CTGCGTAGTTGTGCTGATGT
Cyclin D1	CAATGACCCCGCACGATTTC	CATGGAGGGCGGATTGGAA
miR-140-3p	CAGTGCTGTACCACAGGGTAGA	TATCCTTGTTCACGACTCCTTCAC
U6	CTCGCTTCGGCAGCACATATACT	ACGCTTCACGAATTTGCGTGTC

OCT4, Octamer-binding transcription factor 4; SOX2, SRY-Box 2; KLF4, Kruppel like factor 4; ABCG2, ATP binding cassette subfamily G member 2; miR, microRNA.

100% methanol at room temperature for 10 min and stained with 1% crystal violet at room temperature for 20 min. All experiments were performed in triplicate.

Caspase-3 activity. Caspase-3 activity was assessed using the Caspase-3 Assay kit according to the manufacturer's protocol (Sigma-Aldrich; Merck KGaA). Briefly, $1x10^6$ A549 or Calu3 cells were lysed following treatment with cisplatin (5 μg/ml) for 24 h at 37˚C in 5% CO_2. Assays were performed in 96-well microtiter plates by incubating 10 μl protein of cell lysate/sample, which was quantified using the bicinchoninic acid assay kit (Pierce; Thermo Fisher Scientific, Inc.), in 80 μl reaction buffer (1% NP-40, 20 mmol/l Tris-HCl [pH 7.5], 137 mmol/l NaCl, and 10% glycerol) supplemented with 10 μl caspase-3 substrate (2 mmol/l Ac-DEVD-pNA). Lysates were incubated at 37˚C for 4 h and caspase-3 activity was subsequently analyzed at a wavelength of 405 nm, using a microplate reader (Bio-Rad Laboratories, Inc.). Caspase-3 activity was determined by calculating the ratio of optical density at 450 nm of the cisplatin treated cells to that of untreated cells. All experiments were performed in triplicate.

Flow cytometric analysis. A549 or Calu3 cells were harvested at a density of $1x10^6$ and washed twice with PBS supplemented with 0.5% BSA fraction V (Gibco; Thermo Fisher Scientific, Inc.) and 2 mM EDTA (Sigma-Aldrich; Merck KGaA), prior to incubation with CD133-phycoerythrin antibody (1:50; cat. no. 372803; BioLegend, Inc.) for 15 min at room temperature. Cells were washed twice with PBS and analyzed using a BD FACSCalibur™ flow cytometer (BD Diagnostics; Becton, Dickinson and Company) and the FlowJo software (version 10; FlowJo, LLC) (34). All experiments were performed in triplicate.

Tumor sphere formation assay. Transfected cells were seeded into six-well ultra-low attachment culture plates (Corning Inc.) at a density of $3x10^3$ cells/well and incubated in DMEM/F12 serum-free medium supplemented with 20 ng/ml EGF, 20 ng/ml bFGF, 5 μg/ml insulin, 0.4% BSA and 2% B-27 (Invitrogen; Thermo Fisher Scientific, Inc.) for 6 days at 37˚C in 5% CO_2. The tumor spheres (diameter >100 μm) were subsequently counted and images were captured with a light microscope (magnification x200; Olympus Corporation) (18).

Western blotting. After transfection for 48 h, total protein was extracted from A549 and Calu3 cells using RIPA lysis buffer (Beyotime Institute of Biotechnology) at 30 min on ice. For nuclear protein extraction, A549 and Calu3 cells were isolated in cell lysis buffer [5 mM PIPES, pH 8.0, 0.85 mM KCl, 0.5% NP40 and 1% protein inhibitor mixture (Sigma-Aldrich; Merck KGaA)] for 30 min on ice and centrifuged at 1,000 x g for 20 min at 4˚C. The supernatant was then removed, where the cell pellet was incubated -1in nuclear lysis buffer [50 mM Tris-HCl, pH 8.0, 10 mM EDTA, 1% SDS and 1% protein inhibitor mixture (Sigma-Aldrich; Merck KGaA)] for 30 min on ice and centrifuged at 10,000 x g for 20 min at 4˚C to isolate the nuclear protein. Protein was quantified using the bicinchoninic acid assay kit (Pierce; Thermo Fisher Scientific, Inc.), according to the manufacturer's protocol and 40 μg protein/lane was separated via SDS-PAGE on a 10% gel. The separated proteins were subsequently transferred onto polyvinylidene fluoride membranes (EMD Millipore) and blocked with Tris Buffered Saline with 0.1% Tween 20 supplemented with 5% non-fat dry milk at room temperature for 1 h. The membranes were incubated with primary antibodies against β-catenin (1:4,000; cat. no. ab32572; Abcam), c-Myc (1:1,000; cat. no. 10828-1-AP; ProteinTech Group, Inc.), cyclin D1 (1:1,000; cat. no. 2978; Cell Signaling Technology, Inc.), GAPDH (1:5,000; cat. no. 60004-1-Ig; ProteinTech Group, Inc.), lamin B1 (1:3,000; cat. no. ab16048; Abcam), p53 (cat. no. 2527, 1:1,000, Cell Signaling Technology, Inc.) and phosphorylated p53 (cat. no. ab1431; 1:1,000; Abcam) overnight at 4˚C. Following the primary incubation, membranes were incubated with a horseradish peroxidase-conjugated goat anti-rabbit secondary antibody (1:4,000; cat. no. ab6721; Abcam) for 1 h at room temperature. Membranes were then washed three times with PBS supplemented with Tween 20 (15 min/wash). Protein bands were visualized using the

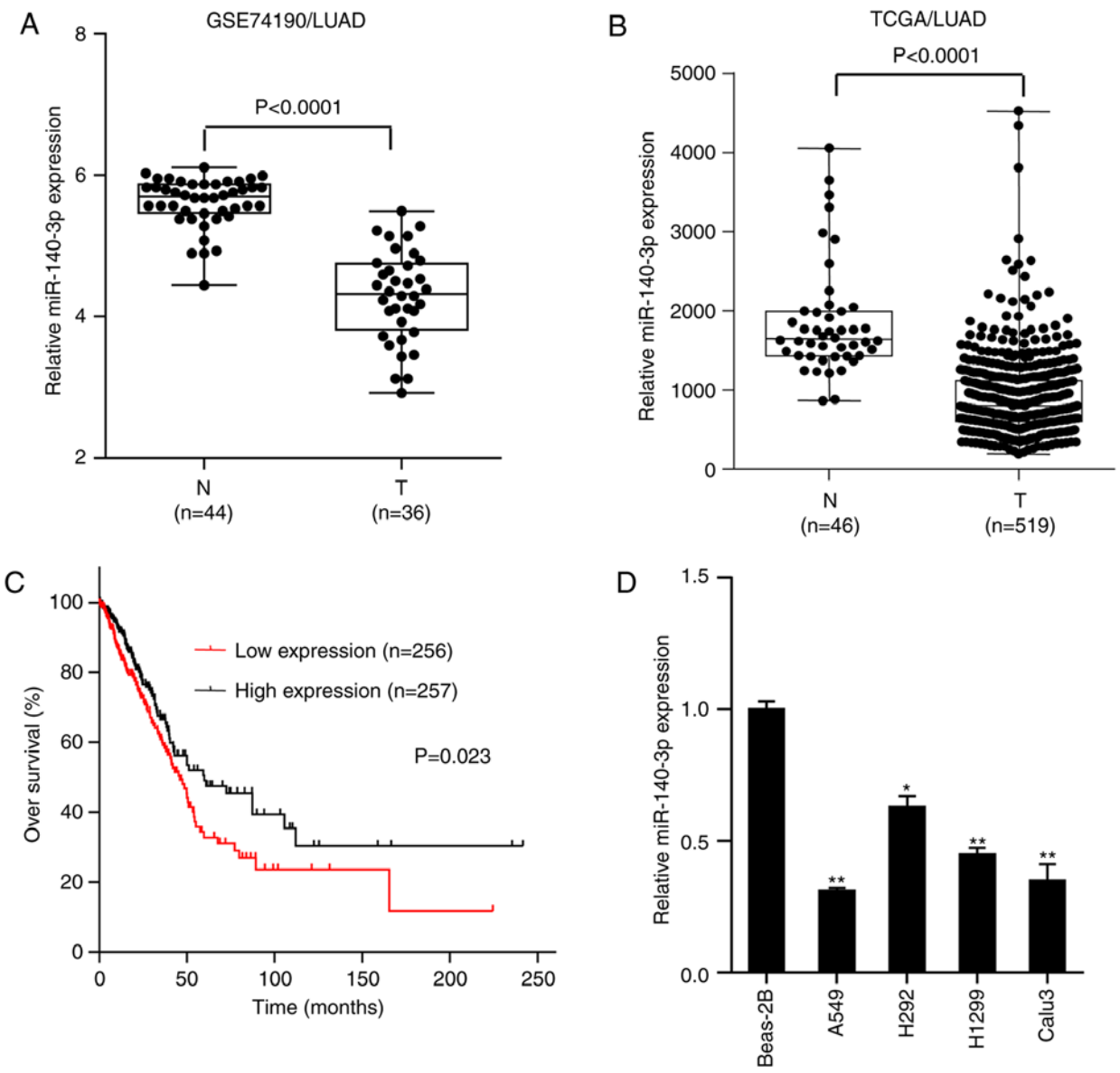

Figure 1. miR-140-3p expression is downregulated in LUAD, which is in turn positively associated with OS of patients. Comparison of miR-140-3p expression between LUAD samples and normal lung tissues in data obtained from the (A) GSE74190 dataset from Gene Expression Omnibus and (B) TCGA database. (C) Kaplan-Meier OS analysis of patients with LUAD, downloaded from TCGA database. (D) Reverse transcription-quantitative PCR analysis of miR-140-3p expression in the lung epithelial cell line BEAS-2B and four LUAD cell lines A549, H292, H1299 and Calu3. Data are presented as the mean ± standard deviation from three independent experiments. *P<0.05 and **P<0.01 vs. BEAS-2B. miR, microRNA; LUAD, lung adenocarcinoma; OS, overall survival; TCGA, The Cancer Genome Atlas; N, normal tissue; T, tumor tissue.

enhanced chemiluminescent substrate kit (Abcam) and Image Lab™ software (version 2.0; Bio-Rad Laboratories, Inc.). Protein expression levels were analyzed using the ImageJ software (version 1.41; National Institutes of Health). GAPDH was used as the internal control.

Dual-luciferase reporter assay. The transcription factor 7 (TCF) reporter assay (TOP/FOP) was performed using the Dual-Glo luciferase assay kit (Promega Corporation), to assess activity of the Wnt/β-catenin signaling pathway. A total of $5x10^4$ A549 or Calu3 cells were seeded into 24-well plates and incubated in RPMI-1640 medium supplemented with 10% FBS and 1% penicillin/streptomycin at 37˚C in 5% CO_2 overnight. Subsequently, cells were co-transfected with 100 ng TOP/FOP flash vector (Promega Corporation), internal control pRL-TK *Renilla* luciferase vector (10 ng) and control mimic or miR-140-3p mimics (50 nM) using Lipofectamine® 2000. After transfection for 48 h, both firefly and *Renilla* luciferase activities were detected in duplicate/triplicate, according to the manufacturer's protocol (35). Firefly luciferase activity was normalized to *Renilla* luciferase activity.

Statistical analysis. Statistical analysis was performed using SPSS software (version 19.0; IBM Corp.). Data are presented as the mean ± standard deviation. Log-rank test was used to determine the statistical significance of Kaplan-Meier overall survival (OS) data of patients. Student's t-test was used to evaluate the differences between two groups, whilst one-way ANOVA followed by Bonferroni post-hoc test was used to measure differences among three groups and a

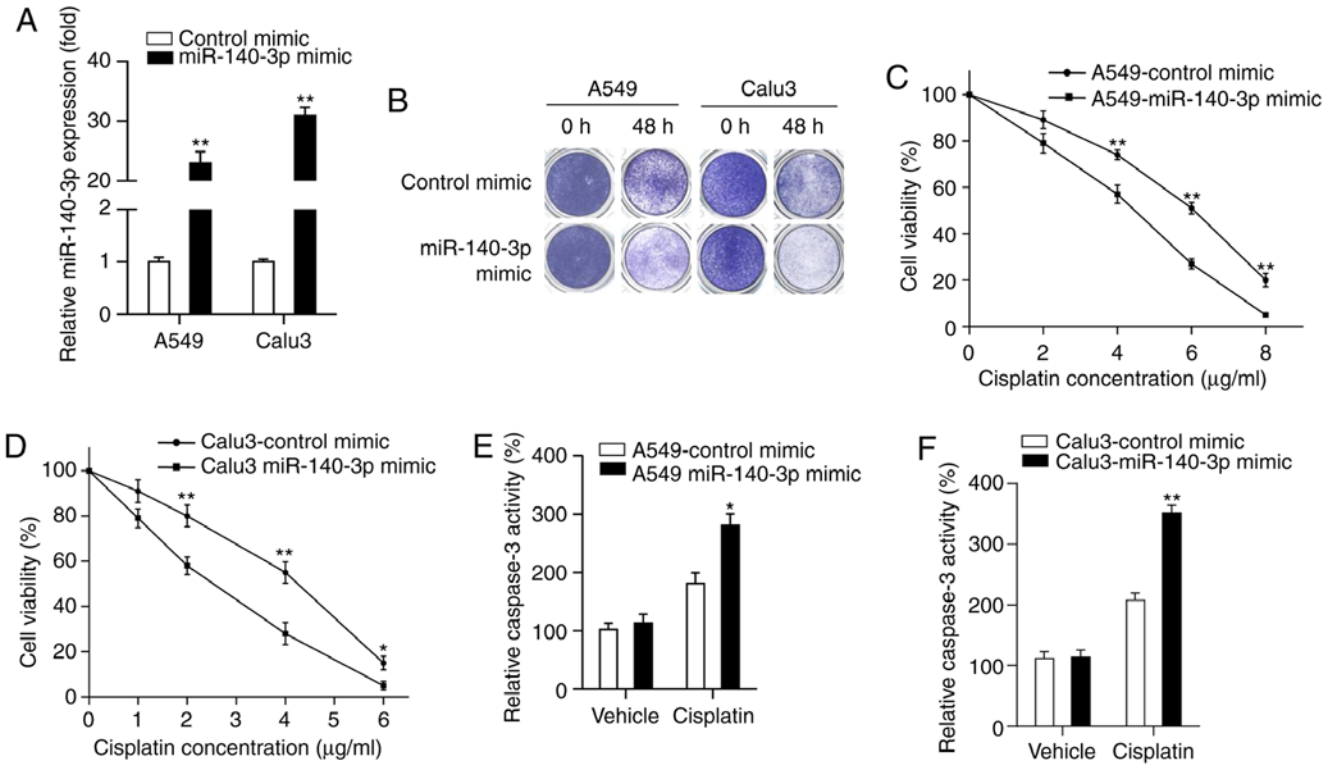

Figure 2. miR-140-3p enhances the sensitivity of LUAD cells to cisplatin. (A) Reverse transcription-quantitative PCR analysis of miR-140-3p expression in the A549 and Calu3 cell lines following transfection with the miR-140-3p mimic or the control mimic. (B) Colony formation of A549 and Calu3 cells following transfection with the miR-140-3p mimic or the control mimic and 5 μg/ml cisplatin treatment. Cell viability of (C) A549 and (D) Calu3 cells as determined by MTT assay, following transfection with the miR-140-3p mimic or the control mimic and then treatment with different concentrations of cisplatin. Caspase-3 activity of (E) A549 and (F) Calu3 cells was determined by caspase-3 assay, following transfection with the miR-140-3p mimic or the control mimic and then treatment with 5 μg/ml cisplatin. All experiments were performed in triplicate and data are presented as the mean ± standard deviation. *P<0.05 and **P<0.01 vs. control mimic. miR, microRNA; LUAD, lung adenocarcinoma.

two-way ANOVA with Bonferroni's correction's was used for between-subject statistical analyses. All experiments were performed in triplicate. P<0.05 was considered to indicate a statistically significant difference.

Results

miR-140-3p is downregulated in LUAD and positively associated with overall survival OS of patients. miR-140-3p expression was assessed in normal lung tissues and LUAD samples in the GSE74190 dataset downloaded from the Gene Expression Omnibus database (https://www.ncbi.nlm.nih.gov/gds/?term). The results demonstrated that miR-140-3p expression was significantly lower in LUAD samples compared with that in normal lung tissues (P<0.0001; Fig. 1A), which was consistent with findings from The Cancer Genome Atlas (TCGA) database (P<0.0001; Fig. 1B). Survival analysis of LUAD data from TCGA database demonstrated that patients with low miR-140-3p expression levels exhibited significantly lower OS rate compared with those with high miR-140-3p expression levels (P=0.023; Fig. 1C). RT-qPCR analysis subsequently indicated that miR-140-3p expression was significantly lower in LUAD cell lines (A549, H292, H1299 and Calu3) compared with human normal bronchial epithelial BEAS-2B cells, particularly in A549 and Calu3 cells (P<0.01; Fig. 1D). These two cell lines (A549 and Calu3) were therefore selected for further experimentation. Taken together, these results suggest that miR-140-3p expression was downregulated in LUAD and positively associated with the OS of patients.

miR-140-3p enhances the sensitivity of LUAD cells to cisplatin. miR-140-3p has been reported to serve as a key tumor suppressor in several types of malignancies, where patients with lower miR-140-3p expression levels had poor prognoses (28-31,33). Therefore, the present study hypothesized that upregulated miR-140-3p expression may be beneficial for the treatment of patients with LUAD. Cisplatin is frequently used as the first-line treatment for NSCLC, which has been reported to improve survival outcomes (6). The effect of miR-140-3p on LUAD cisplatin sensitivity was investigated in the present study. miR-140-3p mimics or control mimics were first transfected into A549 and Calu3 cells, where miR-140-3p expression was significantly higher in the two cell lines transfected with the miR-140-3p mimic compared with those transfected with the control mimic (P<0.01; Fig. 2A). Results from colony formation assay demonstrated that fewer cells survived in the group overexpressing the miR-140-3p mimic treated with cisplatin compared with cells transfected with the control mimic (Fig. 2B). MTT assay indicated that cell viability was significantly decreased in cells transfected with the miR-140-3p mimic treated with different concentrations (A549 cells, 4, 6 and 8 μg/ml; Calu3 cells, 2, 4 and 6 μg/ml) of cisplatin compared with those transfected with the control mimic (P<0.05 and P<0.01; Fig. 2C and D).

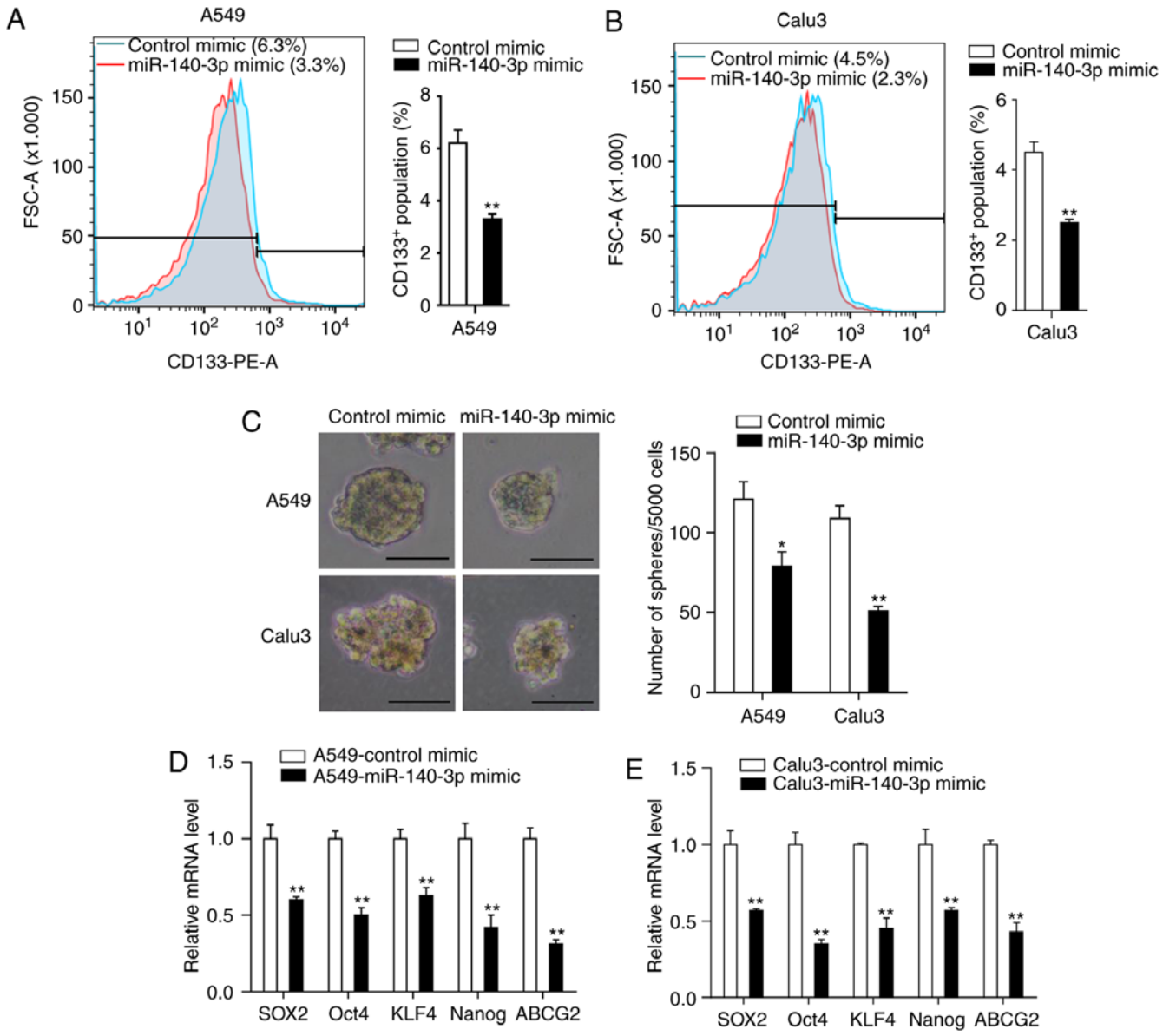

Figure 3. miR-140-3p attenuates the stem cell-like properties of LUAD cells. The percentage of CD133$^+$ cells in (A) A549 and (B) Calu3 cells was analyzed by flow cytometry. (C) Representative images and the number of spheres with diameter >100 μm formed of A549 and Calu3 cells following transfection with miR-140-3p or the control mimic. mRNA expression levels of SOX2, OCT4, KLF4, NANOG and ABCG2 in (D) A549 and (E) Calu3 cells following transfection with miR-140-3p or the control mimic. Data are represented as the mean ± standard deviation from three independent experiments. *P<0.05 and **P<0.01 vs. control mimic. Scale bar, 100 μm. miR, microRNA; LUAD, lung adenocarcinoma; CD133, cluster of differentiation 133; SOX2, SRY-Box 2; OCT4, Octamer-binding transcription factor 4; KLF4, Kruppel like factor 4; ABCG2, ATP binding cassette subfamily G member 2; PE, phycoerythrin; FSC, Forward versus side scatter.

Subsequently, the effect of miR-140-3p on cell apoptosis was measured by assessing caspase-3 activity, following treatment with cisplatin. Caspase-3 activity was found to be significantly increased following miR-140-3p overexpression compared with that in the control mimics group after treatment with cisplatin (P<0.05 and P<0.01; Fig. 2E and F). Collectively, these results suggest that miR-140-3p enhanced sensitivity of LUAD cells to cisplatin.

miR-140-3p decreases stem cell-like properties of LUAD cells. The presence of CSCs is considered a predominant cause of chemoresistance (36). Therefore, the present study investigated the effects of miR-140-3p on the stem cell-like properties in LUAD cells. Flow cytometry analysis of the CSC marker CD133 demonstrated that miR-140-3p overexpression significantly reduced the percentage of CD133$^+$ cells compared with the control mimic group (P<0.01; Fig. 3A and B). Tumor sphere formation assay indicated that cells transfected with the miR-140-3p mimic formed fewer and smaller spheres compared with cells transfected with the control mimic (P<0.05; Fig. 3C). RT-qPCR analysis also demonstrated significantly reduced expression levels of genes associated with stemness (SOX2, OCT4, KLF4, NANOG and ABCG2) in cells overexpressing the miR-140-3p mimic compared cells transfected with the control mimic (P<0.01; Fig. 3D and E). Taken together, these results suggest that miR-140-3p overexpression can attenuate stem cell-like properties of LUAD cells.

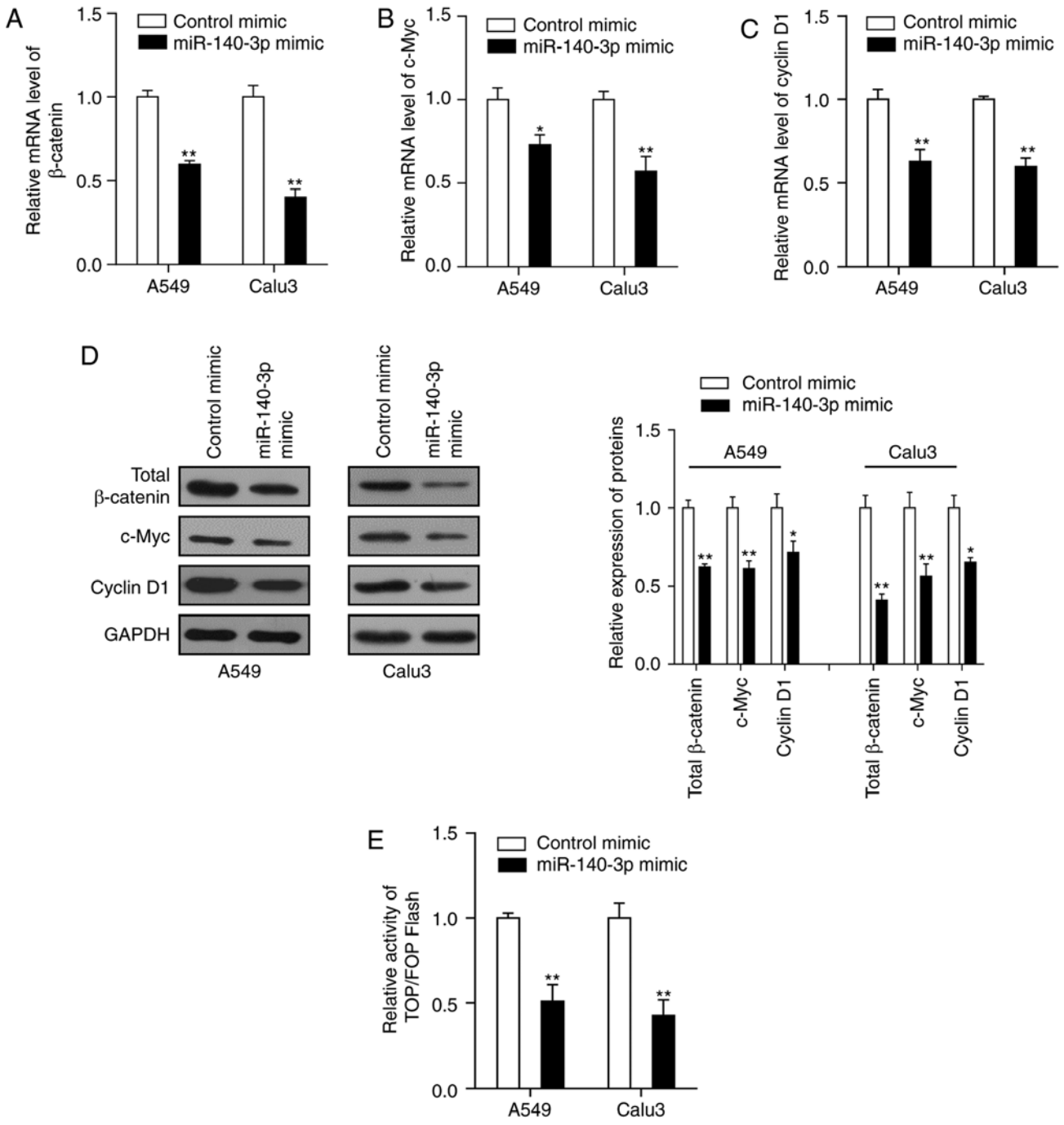

Figure 4. miR-140-3p represses Wnt/β-catenin signaling in LUAD. mRNA expression levels of (A) total β-catenin, (B) c-Myc and (C) cyclin D1 in A549 and Calu3 cells following transfection with miR-140-3p or the control mimic. (D) Protein expression levels of total β-catenin, c-Myc and cyclin D1 following transfection with miR-140-3p or the control mimic. (E) TOP/FOP flash activity in A549 and Calu3 cells following transfection with miR-140-3p or the control mimic. Data are presented as the mean ± standard deviation from three independent experiments. *P<0.05 and **P<0.01 vs. control mimic. miR, microRNA; LUAD, lung adenocarcinoma.

miR-140-3p attenuates the stem cell-like properties and cisplatin resistance in LUAD cells by inhibiting the Wnt/β-catenin signaling. The Wnt/β-catenin signaling pathway is speculated to serve a key role in the self-renewal capacity of CSCs and is activated in several types of human malignancies including LUAD (37). Therefore, the present study hypothesized that upregulated miR-140-3p expression may repress the Wnt/β-catenin signaling, thereby attenuating the stem cell-like properties and cisplatin resistance in LUAD. The results demonstrated that transfection of both LUAD cell lines with the miR-140-3p mimic significantly reduced the mRNA and protein expression levels of β-catenin, c-Myc and cyclin D1 compared with cells transfected with control mimics (P<0.05; Fig. 4A-D). In addition, the dual-luciferase assay suggested that β-catenin/TCF transcriptional activity was significantly reduced in cells co-transfected with miR-140-3p mimic compared with cells transfected with control mimic (P<0.01; Fig. 4E).

The present study investigated whether Wnt/β-catenin signaling mediated the miR-140-3p-attenuated stem cell-like

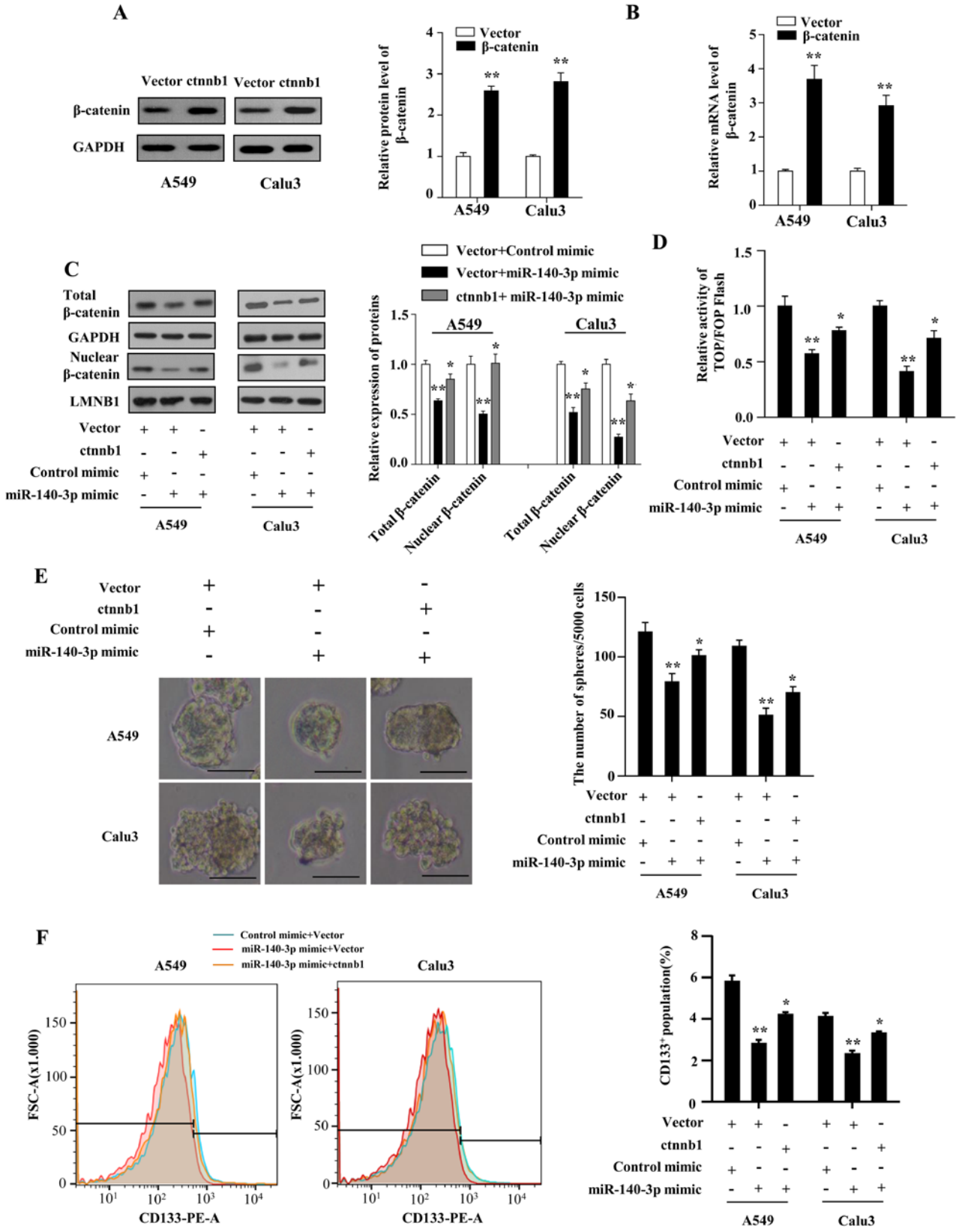

Figure 5. miR-140-3p attenuates the stem cell-like properties in LUAD by suppressing Wnt/β-catenin signaling. (A) Protein and (B) mRNA expression levels of β-catenin in A549 and Calu3 cells following transfection with either the empty vector or vector expressing β-catenin. **P<0.01 vs. vector. (C) Protein levels of total and nuclear β-catenin, *P<0.05 vs. vector + miR-140-3p mimic; **P<0.01 vs. vector + control mimic. (D) TOP/FOP flash activity, *P<0.05 vs. vector + miR-140-3p mimic, **P<0.01 vs. vector + control mimic. (E) number of spheres with diameter >100 μm formed by A549 and Calu3 cells. Scale bar, 100 μm. *P<0.05 vs. vector + miR-140-3p mimic, **P<0.01 vs. vector + control mimic. (F) percentage of CD133^{+}cells analyzed using flow cytometry following co-transfection with either the empty vector or vector expressing β-catenin and miR-140-3p mimic or the control mimic. *P<0.05 vs. vector + miR-140-3p mimic, **P<0.01 vs. vector + control mimic. Data are represented the mean ± standard deviation from three independent experiments. miR, microRNA; LUAD, lung adenocarcinoma; CD133, cluster of differentiation 133; *ctnnb1*, β-catenin gene.

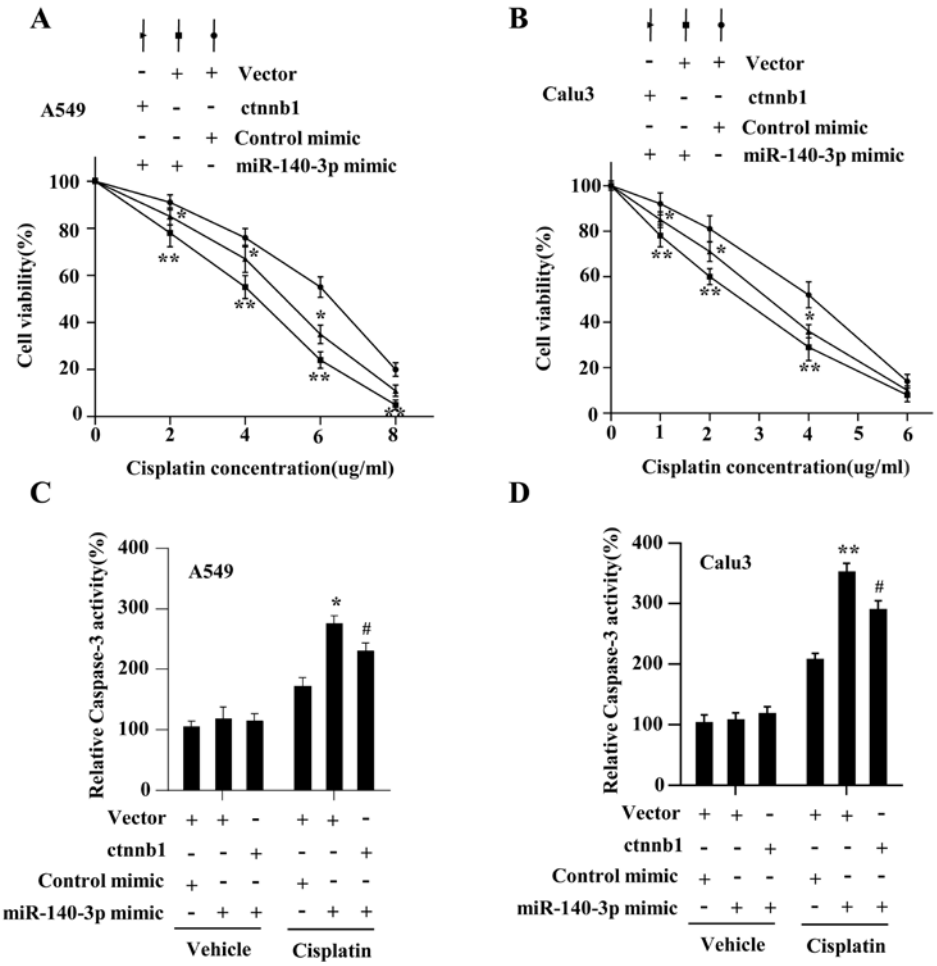

Figure 6. miR-140-3p overexpression enhances cisplatin sensitivity by suppressing Wnt/β-catenin signaling. Cell viability of (A) A549 and (B) Calu3 cells was determined by MTT assay, following co-transfection with either the empty vector or vector expressing β-catenin and miR-140-3p mimic or the control mimic, followed by treatment with different concentrations of cisplatin. *P<0.05 vs. vector + miR-140-3p, **P<0.01 vs. vector + control mimic. Caspase-3 activity of (C) A549 and (D) Calu3 cells was determined using caspase-3 assay, following co-transfection with either the empty vector or vector expressing β-catenin and miR-140-3p mimic or the control mimic, followed by treatment with cisplatin. Data are presented as the mean ± standard deviation from three independent experiments. *P<0.05 vs. vector + control mimic, **P<0.01 vs. vector + control mimic, $^{\#}$P<0.05 vs. vector + miR-140-3p mimic. miR, microRNA; ctnnb1, β-catenin gene.

properties and cisplatin resistance. The results demonstrated that β-catenin expression on both protein and mRNA levels were significantly increased in A549 and Calu3 cells following transfection with plasmids overexpressing β-catenin compared with cells transfected with the vector plasmids (P<0.01; Fig. 5A and B). The levels of total and nuclear β-catenin were found to be restored by co-transfecting the β-catenin plasmid with the miR-140-3p mimic in LUAD cells (P<0.05; Fig. 5C). Co-transfecting LUAD cells with the β-catenin plasmid also significantly reversed the inhibitory effects of miR-140-3p mimics on β-catenin/TCF transcriptional activity (P<0.05; Fig. 5D), $CD133^{+}$ expression (P<0.05; Fig. 5E), sphere formation ability (P<0.05; Fig. 5F). Co-transfection with the β-catenin plasmid also reversed the effects of miR-140-3p on cell viability and antiapoptotic ability, in response to cisplatin treatment (P<0.05; Fig. 6A-D). In addition, the status of p53 in the assessed LUAD cell lines were investigated further but no significant difference was found between cells transfected with the miR-140-3p mimic and those transfected with the control mimic at protein level (data not shown), suggesting that these phenotypic changes mediated by miR-140-3p are p53-independent. Taken together, these results suggest that miR-140-3p attenuated stem cell-like properties and cisplatin resistance in LUAD by repressing the Wnt/β-catenin signaling.

Discussion

Increasing evidence suggests that miRNAs serve key roles in regulating NSCLC progression, therapeutic resistance and stem cell-like properties, all of which constitute an obstacle to the successful treatment of NSCLC (25,38,39). The present study investigated the significance of miR-140-3p expression in LUAD. Based on publicly available data from the GEO and TCGA databases, the results demonstrated that miR-140-3p expression was significantly lower in LUAD samples compared with normal lung tissues, which was found to be positively associated with patient survival, suggesting that miR-140-3p may function as an effective prognostic marker for patients with LUAD.

Although cisplatin is applied extensively for treating LUAD (40), chemotherapy resistance continues to be a major

challenge. Therefore, increasing the cisplatin sensitivity of LUAD cells can serve as a useful therapeutic strategy. Huang *et al* (32) previously reported that miR-140-3p served as a tumor suppressor in LUSC, whilst Li *et al* (30) demonstrated that miR-140-3p enhanced the sensitivity of hepatocellular carcinoma cells to sorafenib. Therefore, the present study hypothesized that miR-140-3p may regulate the development of cisplatin sensitivity in LUAD. The combined results of the colony formation, MTT and caspase-3 assays demonstrated that upregulation of miR-140-3p expression enhanced the sensitivity of LUAD cells to cisplatin. Accumulating evidence supports the hypothesis that CSCs contribute to one of the major mechanisms of tumor cell chemoresistance (41,42). Therefore, the stem cell-like properties of LUAD cells were also investigated in the present study. The results indicated that upregulating miR-140-3p expression reduced the $CD133^+$ cell population, attenuated tumor sphere formation and decreased the expression of pluripotency factors in LUAD cells. Taken together, these results suggest that miR-140-3p may serve a key role in regulating sensitivity to cisplatin and the stem cell-like properties of LUAD cells, thereby acting as a therapeutic target in LUAD.

Over the past few decades, key pathways involved in maintaining cancer stem cell-like properties, including the Wnt/β-catenin, Notch and Hedgehog signaling pathways, have garnered widespread attention (43,44). In particular, the Wnt/β-catenin signaling pathway has become prominent in studies involving NSCLC, since targeting this signaling pathway has been demonstrated to improve anti-CSC-based treatment efficacy (18). Therefore, the present study investigated the effects of miR-140-3p on activation of the Wnt/β-catenin signaling pathway. It was found that the upregulation of miR-140-3p repressed Wnt/β-catenin signaling activation, whilst reactivation of Wnt/β-catenin signaling by β-catenin overexpression partially restored cisplatin resistance and cancer stem cell-like properties of LUAD cells. In addition, considering that the tumor suppressor p53 appears to be at the center of tumor-associated events, including stemness and treatment resistance (45,46), the present study further investigated the status of p53 in the assessed LUAD cell lines, though no significant difference was observed between cells transfected with the miR-140-3p mimic and control mimic at protein level (data not shown), suggesting that these phenotypic changes mediated by miR-140-3p are p53-independent. Taken together, results of the present study indicate that miR-140-3p/Wnt/β-catenin signaling had a notable effect on cancer stem cell-like properties, which may serve a novel regulatory role in the development of cisplatin resistance in patients with LUAD.

The present study had certain limitations. Despite concluding that miR-140-3p expression was downregulated in LUAD, it lacked sufficient data to prove the abnormal expression of miR-140-3p in cisplatin-resistant patient tissues or cell lines. Despite demonstrating that miR-140-3p was positively associated with OS of patients with LUAD, whether miR-140-3p affects the prognosis of patients following treatment with cisplatin requires further investigation.

To the best of our knowledge, the present study was the first to demonstrate that miR-140-3p enhanced cisplatin sensitivity and attenuated stem cell-like properties, by repressing Wnt/β-catenin signaling in LUAD cells. Taken together, results of the present study suggest that miR-140-3p may serve a role as an effective treatment target, whereby targeting miR-140-3p may increase the efficacy of cisplatin in patients with LUAD.

Acknowledgements

Not applicable.

Funding

The present study was funded by the Key R & D Plan of Lianyungang High-tech Zone (grant no. ZD201928).

Availability of data and materials

The datasets used and/or analyzed during the current study are available from the corresponding author on reasonable request.

Authors' contributions

SW and DW designed the experiments and wrote the manuscript. SW and HW performed the experiments. YP and XY contributed to data analysis. All authors read and approved the final manuscript.

Ethics approval and consent to participate

Not applicable.

Patient consent for publication

Not applicable.

Competing interests

The authors declare that they have no competing interests.

References

1. Travis WD, Brambilla E, Nicholson AG, Yatabe Y, Austin JHM, Beasley MB, Chirieac LR, Dacic S, Duhig E, Flieder DB, *et al*: The 2015 world health organization classification of lung tumors: Impact of genetic, clinical and radiologic advances since the 2004 classification. J Thorac Oncol 10: 1243-1260, 2015.
2. Siegel RL, Miller KD and Jemal A: Cancer statistics, 2018. CA Cancer J Clin 68: 7-30, 2018.
3. Ferlay J, Soerjomataram I, Dikshit R, Eser S, Mathers C, Rebelo M, Parkin DM, Forman D and Bray F: Cancer incidence and mortality worldwide: Sources, methods and major patterns in GLOBOCAN 2012. Int J Cancer 136: E359-E386, 2015.
4. Siegel RL, Miller KD and Jemal A: Cancer statistics, 2017. CA Cancer J Clin 67: 7-30, 2017.
5. Han L, Xu G, Xu C, Liu B and Liu D: Potential prognostic biomarkers identified by DNA methylation profiling analysis for patients with lung adenocarcinoma. Oncol Lett 15: 3552-3557, 2018.
6. Fennell DA, Summers Y, Cadranel J, Benepal T, Christoph DC, Lal R, Das M, Maxwell F, Visseren-Grul C and Ferry D: Cisplatin in the modern era: The backbone of first-line chemotherapy for non-small cell lung cancer. Cancer Treat Rev 44: 42-50, 2016.
7. Chang A: Chemotherapy, chemoresistance and the changing treatment landscape for NSCLC. Lung Cancer 71: 3-10, 2011.

8. Zarogoulidis P, Petanidis S, Kioseoglou E, Domvri K, Anestakis D and Zarogoulidis K: MiR-205 and miR-218 expression is associated with carboplatin chemoresistance and regulation of apoptosis via Mcl-1 and survivin in lung cancer cells. Cell Signal 27: 1576-1588, 2015.
9. Tian H, Liu S, Zhang J, Zhang S, Cheng L, Li C, Zhang X, Dail L, Fan P, Dai L, *et al*: Enhancement of cisplatin sensitivity in lung cancer xenografts by liposome-mediated delivery of the plasmid expressing small hairpin RNA targeting survivin. J Biomed Nanotechnol 8: 633-641, 2012.
10. Zhang Y, Yuan Y, Li Y, Zhang P, Chen P and Sun S: An inverse interaction between HOXA11 and HOXA11-AS is associated with cisplatin resistance in lung adenocarcinoma. Epigenetics 14: 949-960, 2019.
11. Li J, Wang Y, Song Y, Fu Z and Yu W: MiR-27a regulates cisplatin resistance and metastasis by targeting RKIP in human lung adenocarcinoma cells. Mol Cancer 13: 193, 2014.
12. Zhan J, Wang P, Li S, Song J, He H, Wang Y, Liu Z, Wang F, Bai H, Fang W, *et al*: HOXB13 networking with ABCG1/EZH2/Slug mediates metastasis and confers resistance to cisplatin in lung adenocarcinoma patients. Theranostics 9: 2084-2099, 2019.
13. Clarke MF, Dick JE, Dirks PB, Eaves CJ, Jamieson CH, Jones DL, Visvader J, Weissman IL and Wahl GM: Cancer stem cells-perspectives on current status and future directions: AACR workshop on cancer stem cells. Cancer Res 66: 9339-9344, 2006.
14. Visvader JE and Lindeman GJ: Cancer stem cells in solid tumours: Accumulating evidence and unresolved questions. Nat Rev Cancer 8: 755-768, 2008.
15. Lathia J, Liu H and Matei D: The clinical impact of cancer stem cells. Oncologist 17: 0517, 2019.
16. Bora-Singhal N, Mohankumar D, Saha B, Colin CM, Lee JY, Martin MW, Zheng X, Coppola D and Chellappan S: Novel HDAC11 inhibitors suppress lung adenocarcinoma stem cell self-renewal and overcome drug resistance by suppressing Sox2. Sci Rep 10: 4722, 2020.
17. Eramo A, Lotti F, Sette G, Pilozzi E, Biffoni M, Di Virgilio A, Conticello C, Ruco L, Peschle C and De Maria R: Identification and expansion of the tumorigenic lung cancer stem cell population. Cell Death Differ 15: 504-514, 2008.
18. Lu CH, Yeh DW, Lai CY, Liu YL, Huang LR, Lee AY, Jin SC and Chuang TH: USP17 mediates macrophage-promoted inflammation and stemness in lung cancer cells by regulating TRAF2/TRAF3 complex formation. Oncogene 37: 6327-6340, 2018.
19. Chiou SH, Wang ML, Chou YT, Chen CJ, Hong CF, Hsieh WJ, Chang HT, Chen YS, Lin TW, Hsu HS and Wu CW: Coexpression of oct4 and nanog enhances malignancy in lung adenocarcinoma by inducing cancer stem cell-like properties and epithelial-mesenchymal transdifferentiation. Cancer Res 70: 10433-10444, 2010.
20. Donnenberg VS and Donnenberg AD: Multiple drug resistance in cancer revisited: The cancer stem cell hypothesis. J Clin Pharmacol 45: 872-877, 2005.
21. Takebe N, Miele L, Harris PJ, Jeong W, Bando H, Kahn M, Yang SX and Ivy SP: Targeting notch, hedgehog, and Wnt pathways in cancer stem cells: Clinical update. Nat Rev Clin Oncol 12: 445-464, 2015.
22. Chatterjee S and Sil PC: Targeting the crosstalks of Wnt pathway with hedgehog and notch for cancer therapy. Pharmacol Res 142: 251-261, 2019.
23. Park EY, Chang E, Lee EJ, Lee HW, Kang HG, Chun KH, Woo YM, Kong HK, Ko JY, Suzuki H, *et al*: Targeting of miR34a-NOTCH1 axis reduced breast cancer stemness and chemoresistance. Cancer Res 74: 7573-7582, 2014.
24. Bitarte N, Bandres E, Boni V, Zarate R, Rodriguez J, Gonzalez-Huarriz M, Lopez I, Javier Sola J, Alonso MM, Fortes P and Garcia-Foncillas J: MicroRNA-451 is involved in the self-renewal, tumorigenicity, and chemoresistance of colorectal cancer stem cells. Stem Cells 29: 1661-1671, 2011.
25. Wang X, Meng Q, Qiao W, Ma R, Ju W, Hu J, Lu H, Cui J, Jin Z, Zhao Y and Wang Y: MiR-181b/Notch2 overcome chemoresistance by regulating cancer stem cell-like properties in NSCLC. Stem Cell Res Ther 9: 327, 2018.
26. Liu T, Wu X, Chen T, Luo Z and Hu X: Downregulation of DNMT3A by miR-708-5p inhibits lung cancer stem cell-like phenotypes through repressing Wnt/β-catenin signaling. Clin Cancer Res 24: 1748-1760, 2018.
27. Sun T, Song Y, Yu H and Luo X: Identification of lncRNA TRPM2-AS/miR-140-3p/PYCR1 axis's proliferates and anti-apoptotic effect on breast cancer using co-expression network analysis. Cancer Biol Ther 20: 760-773, 2019.
28. Zhang QY, Men CJ and Ding XW: Upregulation of microRNA-140-3p inhibits epithelial-mesenchymal transition, invasion, and metastasis of hepatocellular carcinoma through inactivation of the MAPK signaling pathway by targeting GRN. J Cell Biochem 120: 14885-14898, 2019.
29. Zhou Y, Wang B, Wang Y, Chen G, Lian Q and Wang H: MiR-140-3p inhibits breast cancer proliferation and migration by directly regulating the expression of tripartite motif 28. Oncol Lett 17: 3835-3841, 2019.
30. Li J, Zhao J, Wang H, Li X, Liu A, Qin Q and Li B: MicroRNA-140-3p enhances the sensitivity of hepatocellular carcinoma cells to sorafenib by targeting pregnenolone X receptor. Onco Targets Ther 11: 5885-5894, 2018.
31. Tan X, Qin W, Zhang L, Hang J, Li B, Zhang C, Wan J, Zhou F, Shao K, Sun Y, *et al*: A 5-microRNA signature for lung squamous cell carcinoma diagnosis and hsa-miR-31 for prognosis. Clin Cancer Res 17: 6802-6811, 2011.
32. Huang H, Wang Y, Li Q, Fei X, Ma H and Hu R: MiR-140-3p functions as a tumor suppressor in squamous cell lung cancer by regulating BRD9. Cancer Lett 446: 81-89, 2019.
33. Livak KJ and Schmittgen TD: Analysis of relative gene expression data using real-time quantitative PCR and the 2(-Delta Delta C(T)) method. Methods 25: 402-408, 2001.
34. Cao S, Wang Z, Gao X, He W, Cai Y, Chen H and Xu R: FOXC1 induces cancer stem cell-like properties through upregulation of beta-catenin in NSCLC. J Exp Clin Cancer Res 37: 220, 2018.
35. Cui Y, Ma W, Lei F, Li Q, Su Y, Lin X, Lin C, Zhang X, Ye L, Wu S, *et al*: Prostate tumour overexpressed-1 promotes tumourigenicity in human breast cancer via activation of Wnt/β-catenin signalling. J Pathol 239: 297-308, 2016.
36. MacDonagh L, Gray SG, Breen E, Cuffe S, Finn SP, O'Byrne KJ and Barr MP: Lung cancer stem cells: The root of resistance. Cancer Lett 372: 147-156, 2016.
37. Jiang N, Zou C, Zhu Y, Luo Y, Chen L, Lei Y, Tang K, Sun Y, Zhang W, Li S, *et al*: HIF-1a-regulated miR-1275 maintains stem cell-like phenotypes and promotes the progression of LUAD by simultaneously activating Wnt/β-catenin and notch signaling. Theranostics 10: 2553-2570, 2020.
38. Li T, Ding ZL, Zheng YL and Wang W: MiR-484 promotes non-small-cell lung cancer (NSCLC) progression through inhibiting apaf-1 associated with the suppression of apoptosis. Biomed Pharmacother 96: 153-164, 2017.
39. Ma Z, Cai H, Zhang Y, Chang L and Cui Y: MiR-129-5p inhibits non-small cell lung cancer cell stemness and chemoresistance through targeting DLK1. Biochem Biophys Res Commun 490: 309-316, 2017.
40. Zhang Y, Du H, Li Y, Yuan Y, Chen B and Sun S: Elevated TRIM23 expression predicts cisplatin resistance in lung adenocarcinoma. Cancer Sci 111: 637-646, 2020.
41. Chen MJ, Wu DW, Wang YC, Chen CY and Lee H: PAK1 confers chemoresistance and poor outcome in non-small cell lung cancer via beta-catenin-mediated stemness. Sci Rep 6: 34933, 2016.
42. MacDonagh L, Gray SG, Breen E, Cuffe S, Finn SP, O'Byrne KJ and Barr MP: BBI608 inhibits cancer stemness and reverses cisplatin resistance in NSCLC. Cancer Lett 428: 117-126, 2018.
43. Lathia JD and Liu H: Overview of cancer stem cells and stemness for community oncologists. Targeted Oncol 12: 387-399, 2017.
44. Najafi M, Farhood B and Mortezaee K: Cancer stem cells (CSCs) in cancer progression and therapy. J Cell Physiol 234: 8381-8395, 2019.
45. Fu X, Wu S, Li B, Xu Y and Liu J: Functions of p53 in pluripotent stem cells. Protein Cell 11: 71-78, 2020.
46. Cao X, Hou J, An Q, Assaraf YG and Wang X: Towards the overcoming of anticancer drug resistance mediated by p53 mutations. Drug Resist Updat 49: 100671, 2019.